https://doi.org/10.1016/j.trc.2019.06.009

Surrogate-based Simulation Optimization Approach for Day-to-day Dynamics Model Calibration with Real Data

Qixiu Cheng [a], Shuaian Wang [b], Zhiyuan Liu [a], Yu Yuan [a]*

[a] Jiangsu Key Laboratory of Urban ITS, Jiangsu Province Collaborative Innovation Center of Modern Urban Traffic Technologies, School of Transportation, Southeast University, China

[b] Department of Logistics & Maritime Studies, The Hong Kong Polytechnic University, Kowloon, Hong Kong

**Corresponding author. Email address: zhiyuanl@seu.edu.cn (Z. Liu)*

Abstract: This paper investigates the day-to-day dynamics model from the perspective of travelers' actual route choice behaviors, and calibrates and validates the route-based day-to-day dynamics model with the real-world license plate recognition (LPR) data. Due to the highly nonlinear and multi-modal response function in the calibration of the optimization problem, traditional gradient-based nonlinear regression algorithms or other analytical optimization approaches are inapplicable to deal with the calibration work. In this paper, a surrogate-based simulation optimization approach is proposed to deal with the expensive-to-evaluate response function in the day-to-day dynamics calibration work. More specifically, the kriging metamodel is adopted to surrogate the optimization function of the calibration process. With this meta-modeling approach, a sound solution can be achieved with only a few sampling points in a comfortably afforded computation burden, thus giving a valid estimation of the parameters in the day-to-day dynamics model. Finally, a case study based on the real-world LPR data is conducted to validate the proposed model and calibration method.

Keywords: Traffic; Calibration; Day-to-day dynamics; Simulation-based optimization; License plate recognition (LPR) data

1 Introduction

Traffic assignment problem is the last step of the classical four-step transportation forecasting model, which is a special case of the most general partial share demand modeling approach. Conventional traffic assignment approaches assume that the network characteristics (e.g., road capacity and infrastructure construction) and the traffic demand keep unchanged for a relatively extended period. However, a stable equilibrium state may never be achieved in real life due to the variation of network demand and infrastructure during the planning period. The traffic dynamics model that focuses on the one-shot final stable equilibrium state is usually classed as the within-day dynamics model. The within-day dynamics model can be dated back to Merchant and Nemhauser (1978a, 1978b) and since then a lot of researches are focused on this area, and interested readers are referred to Peeta and Ziliaskopoulos (2001), Szeto and Lo (2006), Mun (2007) for a comprehensive review. In contrast, another type of dynamic traffic assignment patterns, termed as day-to-day dynamics models, takes into consideration the network evolution over days, and road users can learn from the past experiences and adjust their route choice behaviors from day to day during this period. The day-to-day dynamics model can be traced back to Horowitz (1984), Smith (1984), Cascetta (1989), Cascetta and Cantarella (1991), Friesz et al. (1994), Cantarella and Cascetta (1995), just to name a few. Recently, the day-to-day dynamics models have been applied to model the unexpected network disruption (He and Liu, 2012), dynamic congestion pricing (Liu et al., 2017), adaptive pricing with park-and-ride (Liu and Geroliminis, 2017), design of transit operator strategies (Cantarella et al., 2015), urban railway network (Wu et al., 2013) and intelligent transportation systems (Cantarella, 2013), etc.

Day-to-day dynamics models are essential to describe travelers' route choice and route switching behaviors each day; inevitably the route adjustment ratio is vital for all of the day-to-day dynamics models. All the existing day-to-day dynamics models are approached either theoretically or experimentally. From a theoretical point of view, the day-to-day dynamics is formulated as the evolution process of the network state variables (including link/route flows and costs) over successive time periods such as days or weeks, either as a deterministic (e.g. Guo et al., 2016) or stochastic (e.g. Cantarella and Watling, 2016) process, in continuous (e.g. He et al., 2010) or discrete (e.g. Cantarella, 2013) time. The focus of many existing studies is

on the theoretical issues such as the convergence of defined dynamic processes and stability properties of the network equilibrium, rather than implementation ones like the calibration against observed data. They usually take a plausible constant as the route adjustment ratio, leading to the lack of practical application value of these models. As for experimental analysis (e.g., Meneguzzer and Olivieri, 2013; Ye et al., 2018), the day-to-day dynamics models observe travelers' route choice directly and route switching behaviors over time. However, the experimental analysis of day-to-day dynamics is based on the laboratory-like or simulated-based controlled experiments with hypothetical choice situations and a limited number of participants in simple networks. Therefore, it is an emerging research need to investigate the day-to-day dynamics from travelers' actual travel behaviors and to calibrate and validate the day-to-day dynamics with real-world data.

License plate recognition (LPR) data are burgeoning and useful data sources in urban and highway transportation systems (Zhan et al., 2015). LPR data are widely used in the electronic toll collection systems, traffic monitoring systems and law enforcement systems. The recorded information of LPR data is abundant, including the vehicle license plate number, vehicle type, timestamp at the stop lines, instantaneous speed, intersection name, and intersection number, etc. For example, according to the Ministry of Public Security (2016), the recognition accuracy of the license plate number in China should be no less than 95% in the daytime, and no less than 90% in the nighttime. Such a high recognition accuracy makes it suitable to use the LPR data to re-identify the same vehicle through successive intersections. Specifically, the LPR cameras record the license plate numbers and timestamp sequences for all passing vehicles departing from the stop line of the road, and we can trace the same vehicle between upstream and downstream intersections regarding the license plate number and timestamp sequence. Thus the trajectories of vehicles can be acquired. In this study, we will take full advantages of the LPR data to investigate the day-to-day dynamics of route choice and route switching behaviors, and calibrate as well as validate the day-to-day dynamics with LPR data.

The calibration of day-to-day dynamics model is extremely complicated to deal with because of the highly nonlinear and multi-modal response function in the optimization problem (as shown in Section 3.2). For example, when we calculate the response for a particular input variable, we need to first obtain the traffic flows and costs from the first day to the last day in

terms of the flow and cost updating processes in the day-to-day dynamics model without a closed-form function, which is a tedious work especially when the network size is large-scale and the period is long-term. Therefore, the calibration of day-to-day dynamics model cannot be handled with the gradient-based nonlinear regression algorithms or other analytical optimization approaches. In order to solve this complicated problem, we use a surrogate-based simulation optimization approach to deal with the expensive-to-evaluate response function[1]. More specifically, the kriging metamodel is adopted to surrogate the optimization function of the calibration process. With this meta-modeling approach, a sound solution can be achieved with only a few sampling points in a comfortably afforded computation burden, thus giving a valid estimation of the parameters in the day-to-day dynamics model.

1.1 Literature review

The day-to-day dynamics model is one category of the dynamic traffic assignment models describing the network flow evolutionary process and has been extensively studied since Horowitz (1984) and Smith (1984). The day-to-day dynamics model can be formulated as either deterministic process models with the steady state of user equilibrium (e.g., Smith, 1984; Smith and Wisten, 1995; Cho and Hwang, 2005; Yang and Zhang, 2009; Bie and Lo, 2010; Cantarella and Watling, 2016), stochastic user equilibrium (e.g., Cantarella and Cascetta, 1995; Smith and Watling, 2016) and boundedly rational user equilibrium (e.g., Mahmassani and Chang, 1987; Guo and Liu, 2011; Wu et al., 2013; Di et al., 2015; Ye and Yang, 2017); or stochastic process models with the steady state as the equilibrium probability distribution (e.g., Cascetta, 1987, 1989; Cascetta and Cantarella, 1991; Davis and Nihan, 1993; Hazelton, 2002; Hazelton and Watling, 2004; Parry and Hazelton, 2013; Watling and Cantarella, 2013; Watling and Cantarella, 2015; Hazelton and Parry, 2016).

However, as claimed in Mahmassani (1990), the difficulty of day-to-day dynamic traffic assignment model is to verify the day-to-day evolutionary process based on real-world observed data. Some studies investigated the influencing factors (such as information, experience, risk, uncertainty, etc) of day-to-day dynamics with simulation and laboratory-like experiments (e.g., Mahmassani and Chang, 1986; Mahmassani, 1990; Hu and Mahmassani, 1997; Lotan, 1997;

[1] It should be noted that the concept of 'simulation' here refers to a random observation of the network systems.

Mahmassani and Jou, 2000; Srinivasan and Mahmassani, 2003; Avineri and Prashker, 2005; Lu et al., 2011; Ben-Elia et al., 2013; just to name a few). However, the calibration of the day-to-day dynamics model is sparse. He and Liu (2012) modeled the day-to-day dynamic traffic flow evolutionary process with a prediction-correlation model in a link-based approach. Their proposed model is calibrated and validated based on the field data after the collapse of I-35W Mississippi River Bridge in Minneapolis, Minnesota. On the contrary, Meneguzzer and Olivieri (2013) calibrated a route-based day-to-day dynamics model based on a laboratory-like experiment with 30 participants. Ye et al. (2018) also calibrated the parameters of different route-based day-to-day dynamics models based on a virtual experiment with 268 participants in a three-path network. However, in many existing studies, the route choice behaviors of day-to-day dynamics were not considered, and also the network size and number of participants were restricted with controlled experiments. In this paper, we will bridge these gaps and calibrate the route-based day-to-day dynamics model with real-world LPR data, which can better reflect the actual route choice and route change behaviors from day to day.

The simulation-based optimization approach has also been widely used to solve the problems of congestion pricing (Chen et al., 2016; He et al., 2017), traffic signal control (Chong and Osorio, 2015; Osorio and Bierlaire, 2013; Osorio and Nanduri, 2015a, 2015b), transit scheduling (Zhang and Xu, 2017), vehicle sharing (Cardin et al., 2017), supply chain management (Noordhoek et al., 2018), liner shipping (Dong and Song, 2009), etc. In general, there are three classes of methods for the simulation-based optimization, including the direct-search method, the stochastic gradient method, and the metamodel (or surrogate) method (Osorio and Bierlaire, 2013). Among these methods, the metamodel method is favored due to the determinacy of the metamodel response(s), thus making it computationally more efficient than other methods. The metamodel is an approximated model that is inexpensive to compute to describe the original model with the complicated and computationally expensive response(s). The metamodel method includes the response surface method, the regression spline method, the spatial correlation (also known as the kriging) method, the radial basis function (RBF) method, and the neural network method (Barton and Meckesheimer, 2006; Chen, 2017). The similarity of these models is that they are approximated models, rather than exact optimization models. The differences are mainly in the approximating functions: 1) the response surface

method uses *first or second order polynomial probability models* to fit the system response; 2) the regression spline method uses *piecewise polynomial basis functions* to fit the objective function; 3) the spatial correlation method, which is also known as the kriging method, estimates the interpolated function values based on a *Gaussian process* governed by the covariance of previously known data; 4) the radial basis function (RBF) method approximates the response with *a series of radially symmetric functions* whose center are at different points; and 5) the neural network method typically approximates the response with *multi-layer neural networks* and now is widely used in artificial intelligence and machine learning algorithms. For a comprehensive review of the metamodel, we refer readers to Forrester and Keane (2009), Han and Zhang (2012) and Kleijnen (2017).

The kriging model is a widely-used surrogate model (or metamodel). We choose the kriging metamodel in this paper because it is more flexible than polynomial regression models in fitting arbitrary smooth response functions and less sensitive than other meta-models (such as RBF) to a small change in the design of experiment (Barton and Meckesheimer, 2006). The kriging method dates back to the early 1960s in the geology literature (Cressie, 1990), and has been successfully adopted in statistics and global optimization problems (Jones et al., 1998; Sacks et al., 1989). Sacks et al. (1989) proposed a DACE (which is the acronym of design and analysis of computer experiments) algorithm for spatial correlation parametric regression based on kriging method. The DACE algorithm is then extended to an efficient global optimization (EGO) in Jones et al. (1998) by introducing a diagnostic test based on cross-validation and infilling new points with maximization of expected improvement (EI). The outline of the EGO algorithm is summarized as follows: 1) build an easy-to-compute kriging metamodel for the complicated response function; 2) cross-validation; 3) find the new point which maximizes the EI; 4) add the new point, evaluate it and update the kriging metamodel. Interested readers may refer to Kleijnen (2009, 2017) for a comprehensive review of the kriging metamodel.

1.2 Objectives and contributions

This paper aims to investigate the day-to-day traffic flow evolutionary process from the viewpoint of travelers' route choice behaviors, and calibrate and validate the route based day-to-day dynamics model with real-world data. Due to the highly nonlinear and multi-modal

response function in the optimization problem, it is extremely complex to calibrate the parameters in the day-to-day dynamics model, especially when the network size is large-scale and the period is long-term. Thus, a surrogate-based simulation optimization approach is proposed to deal with the expensive-to-evaluate response function. With this surrogate-based simulation optimization approach, the parameters in the route based day-to-day dynamics model can be well calibrated. To sum up, the contributions of this paper are threefold: 1) a surrogate-based simulation optimization approach is proposed to calibrate the classic deterministic process of route based day-to-day dynamic model; 2) the proposed route-based day-to-day dynamics model is validated with the surrogate-based simulation optimization approach based on the real-world license plate recognition data; 3) some insights for the parameters are discussed in this paper.

The paper is organized as follows: Section 2 first introduces the network representation and notations used in this paper and then proposed a general framework of the route based day-to-day dynamics model. Section 3 introduces the methodology, including how to trace vehicles' trajectories with LPR data and the surrogate-based simulation optimization approach for calibrating the route based day-to-day dynamics model. Section 4 conducts a case study with the LPR data obtained in Yuyao City, China to calibrate and validate the route based day-to-day dynamics model and the proposed surrogate-based simulation optimization approach, and analyses the results of the calibration work. Finally, Section 5 concludes this study and gives some future research directions.

2 Problem Description

2.1 Network representation and notations

Consider a general and strongly connected transportation network, which is represented by $G=(N,A)$, where N is the set of nodes and A is the set of directed links. We denote the set of OD pairs by W, the set of paths between OD pair $w\in W$ by K_w, and the demand of OD pair $w\in W$ by q_w. f_{wk} denotes the traffic flow of route $k\in K_w$, and $\boldsymbol{f}_w=(f_{wk},k\in K_w)$. v_a denotes the traffic flow on link $a\in A$, and $\boldsymbol{v}=(v_a,a\in A)$. Let t

denote the time epoch, which is a particular day in the calendar. Then, f_{wk}^t is the traffic flow of route $k \in K_w$ on day t, and $\boldsymbol{f}_w^t = (f_{wk}^t, k \in K_w)$. Other notations in this paper are summarized in Table 1.

Table 1: Summary of the notations used in the day-to-day dynamics model

Notation	Explanations
W	Set of OD pairs
w	OD pair $w \in W$
K_w	Set of routes between OD pair $w \in W$
k	Traffic route $k \in K_w$
q_w	Traffic demand between OD pair $w \in W$
$\boldsymbol{C}_w^t$	Vector of forecasted costs between OD pair w on day t
C_{wk}^t	Forecasted cost of route k between OD pair $w \in W$ on day t
$\boldsymbol{c}_w^t$	Vector of actual costs between OD pair w on day t
c_{wk}^t	Actual cost of route k between OD pair $w \in W$ on day t
$\boldsymbol{f}_w^t$	Vector of route flow between OD pair w on day t
f_{wk}^t	Traffic flow of route k between OD pair $w \in W$ on day t
$\boldsymbol{R}_w^t$	Matrix of route adjustment ratio for OD pair w on day t
$r_{k,j}^t$	Route adjustment ratio, i.e., the portion of travelers choosing route j on day $t-1$ but switching to route k on day t, $\sum_{k \in K_w} r_{k,j}^t = 1, \forall j \in K_w, w \in W$
p_{wk}^t	Choice probability of route k between OD pair $w \in W$ on day t in terms of the utility function
α	Weighting parameter used for adjusting the forecasted cost on the next day
β	Reconsideration ratio, i.e., the portion of travelers who will reconsider the route choice decisions of the previous day in the next day
θ	Dispersion parameter in the logit-type function

2.2 A general framework of route based day-to-day dynamics model

Day-to-day dynamics models are of great value in describing travelers' route choice and route adjustment behaviors from epoch to epoch. To model the evolution process of the day-to-

day dynamics, network state variables of flows and costs can be represented as link-based or route-based models. Link-based day-to-day dynamics models formulate the network evolution process in terms of the link flows and costs, of which the initial values can be easily observed (He et al., 2010; Zhou et al., 2017). However, in a link-based day-to-day dynamics model, the flow adjustment process is reflected with the *aggregated* link flows, which cannot directly observe the route choice and adjustment behavior of travelers. On the contrary, route-based models trace travelers' route choices and model the route adjustment process from day to day, thus can reflect travelers' route choice behavior during the adjustment process. The focus of this paper is on the calibration and validation of day-to-day dynamics from the perspective of user behavior, thus only route-based models are considered here.

Generally, the day-to-day dynamics models involve two aspects: *a*) travelers' learning and forecasting behavior (i.e., cost updating model), and *b*) travelers' route choice updating behavior (i.e., flow updating model). The cost updating model describes how previous experience (mainly refers to the costs of previous days) influences the forecasted cost on the next day, while the flow updating model describes how present choices are influenced by the decisions of previous days and then updates the network flows.

2.2.1 Cost updating model

In principle, the cost updating model can be formulated by a disaggregate assignment model, i.e., the forecasted cost on route $k \in K_w$ of user i on day t depends on the actual and forecasted route costs on previous days, which is expressed as follows:

$$C_{wk}^{i,t} = C(C_{wk}^{i,t-1}, c_{wk}^{i,t-1}, C_{wk}^{i,t-2}, c_{wk}^{i,t-2}, \cdots) \tag{1}$$

$$\boldsymbol{C}_{w}^{i,t} = \boldsymbol{C}(\boldsymbol{C}_{w}^{i,t-1}, \boldsymbol{c}_{w}^{i,t-1}, \boldsymbol{C}_{w}^{i,t-2}, \boldsymbol{c}_{w}^{i,t-2}, \cdots) \tag{2}$$

where the capital $C_{wk}^{i,t}$ and the lowercase $c_{wk}^{i,t}$ represent the forecasted and actual costs on route $k \in K_w$ of user i on day t, respectively, and the bold $\boldsymbol{C}_{w}^{i,t}$ and $\boldsymbol{c}_{w}^{i,t}$ are the vectors of $C_{wk}^{i,t}$ and $c_{wk}^{i,t}$.

As claimed in Cascetta (2009), however, the disaggregate model would be complex for route choice models in terms of the random utility theory, making it not applicable to analyze the aggregated route flows. Therefore, an aggregated route-based model is more suitable. More specifically, in an aggregated cost updating model, the forecasted cost is a function of the actual

and forecasted route costs on the previous days, which can be expressed as follows:

$$C_{wk}^{t} = C(C_{wk}^{t-1}, c_{wk}^{t-1}, C_{wk}^{t-2}, c_{wk}^{t-2}, \cdots) \tag{3}$$

$$\boldsymbol{C}_{w}^{t} = \boldsymbol{C}(\boldsymbol{C}_{w}^{t-1}, \boldsymbol{c}_{w}^{t-1}, \boldsymbol{C}_{w}^{t-2}, \boldsymbol{c}_{w}^{t-2}, \cdots) \tag{4}$$

where the capital C_{wk}^{t} and the lowercase c_{wk}^{t} represent the aggregated forecasted and actual costs of route $k \in K_w$ on day t, respectively, and the bold $\boldsymbol{C}_{w}^{t}$ and $\boldsymbol{c}_{w}^{t}$ are the vectors of C_{wk}^{t} and c_{wk}^{t}.

For the sake of simplicity, the forecasted cost on day t is usually assumed to depend only on the forecasted cost $\boldsymbol{C}_{w}^{t-1}$ and the actual cost $\boldsymbol{c}_{w}^{t-1}$ on day $t-1$:

$$\boldsymbol{C}_{w}^{t} = \boldsymbol{C}(\boldsymbol{C}_{w}^{t-1}, \boldsymbol{c}_{w}^{t-1}) \tag{5}$$

As for the cost function, we assume it only depends on the forecasted cost as well as the actual cost on the previous day. Actually, one can assume that the current day's forecasted cost depends on all of the previous days' route choice, implying that travelers never forget any experiences in the past. Such a model is regarded as an infinite learning process as claimed in Cantarella and Watling (2016). However, the travelers' route choice behaviors are highly influenced by unexpected incidents occurring more recently (Liu et al., 2017). Thus, some other researches (e.g., Cascetta, 1989; Cantarella and Watling, 2016; Liu et al., 2017) assume that travelers' route choice behaviors are only influenced by the most recent days (such as the most recent *m* days), resulting in a finite learning process. Compared to the above mentioned finite learning process model, the cost function adopted in this paper is a special case with *m*=1, and it is also widely assumed in the day-to-day dynamics model (e.g., Bie and Lo, 2010; Davis and Nihan, 1993; Guo et al., 2016; He and Liu, 2012; Hu and Mahmassani, 1997; just to name a few). It should be noted that the model can be easily extended when more than one day's memory is considered. For example, if we consider three days' memory, i.e., $\boldsymbol{C}_{w}^{t} = \sum_{i=1}^{3} \alpha_i \boldsymbol{c}_{w}^{t-i} + (1 - \sum_{i=1}^{3} \alpha_i) \boldsymbol{C}_{w}^{t-1}$, then we need to calibrate two more parameters in the experiment. The length of memory does not influence the framework of other portions in the day-to-day dynamics model.

It is worth noting that Eq. (5) is a recursive equation because the actual costs on days prior to *t*-1 will influence the forecasted cost $\boldsymbol{C}_{w}^{t-1}$, thus the choice behavior on day *t* is still implicitly influenced by the actual costs on days prior to *t*-1. We use an exponential filter to

formulate the cost updating model, that is, the forecasted cost on day t is a convex combination of the actual route cost $\boldsymbol{c}_w^{t-1}$ and the forecasted cost $\boldsymbol{C}_w^{t-1}$ on day $t-1$, which is shown as follows (Cantarella and Cascetta, 1995):

$$\boldsymbol{C}_w^t = \alpha \boldsymbol{c}_w^{t-1} + (1-\alpha)\boldsymbol{C}_w^{t-1} \tag{6}$$

where $\alpha \in (0,1]$ is the weight to adjust the forecasted cost on day t in terms of the actual cost and forecasted cost on day $t-1$.

2.2.2 Flow updating model

The flow updating model reflects the flow evolution process from day to day. In a flow updating model, one of the most important elements is the route adjustment ratio. We denote $r_{k,j}^t$ as the portion of travelers choosing route j on day $t-1$ but switching to route k on day t. For a specific OD pair w, it is obvious that $\sum_{k \in K_w} r_{k,j}^t = 1, \forall j \in K_w$. Then the route flow updating model can be formulated as follows:

$$f_{wk}^t = \sum_{j \in K_w} r_{k,j}^t \cdot f_{wj}^{t-1}, \ \forall k \in K_w, \ \forall w \in W \tag{7}$$

To express it in a vector form, we can obtain the following formulations:

$$\boldsymbol{f}_w^t = \boldsymbol{R}_w^t \cdot \boldsymbol{f}_w^{t-1}, \ \forall w \in W \tag{8}$$

The route adjustment ratio matrix $\mathbf{R}_w^t$ is usually formulated as a function of the forecasted cost in Eq. (6), namely:

$$\boldsymbol{R}_w^t = \boldsymbol{R}(\boldsymbol{C}_w^t) \tag{9}$$

Combining with Eq. (8), the route flow can be obtained as follows:

$$\boldsymbol{f}_w^t = \boldsymbol{R}(\boldsymbol{C}_w^t) \cdot \boldsymbol{f}_w^{t-1} \tag{10}$$

From the perspective of user behavior, when we model the route updating process, there are some travelers who repeat the previous day's route choices without any reconsiderations, while the others reconsider the previous day's choices and decide whether changing to a new route with a probability model. This process can also be captured with an exponential filter model:

$$r_{j,j}^t = \beta \cdot p_{wj}^t + (1-\beta), \ \forall j \in K_w, \ \forall w \in W \tag{11}$$

$$r_{k,j}^t = \beta \cdot \frac{p_{wk}^t}{\sum_{l \in K_w} p_{wl}^t} = \beta p_{wk}^t,\ \forall j \neq k,\ j \in K_w, \forall k \in K_w, \forall w \in W \tag{12}$$

where β is the reconsideration ratio, i.e., the portion of travelers who will reconsider the previous route choice decisions, and p_{wk}^t is the route choice probability that a traveler who chooses route $k \in K_w$ on day t in terms of the Eq. (16) discussed later. We can see that the flow conservation condition still holds:

$$\begin{aligned}
\sum_{k \in K_w} r_{k,j}^t &= r_{j,j}^t\Big|_{j \in K_w} + \sum_{\substack{k \neq j \\ k \in K_w}} r_{k,j}^t \\
&= \beta \cdot p_{wj}^t\Big|_{j \in K_w} + (1-\beta) + \beta \cdot \sum_{\substack{k \neq j \\ k \in K_w}} p_{wk}^t \\
&= \beta \cdot \sum_{k \in K_w} p_{wk}^t + (1-\beta) \\
&= \beta + (1-\beta) \\
&= 1
\end{aligned} \tag{13}$$

With the above discussion, the route flow updating model can be reformulated as:

$$\begin{aligned}
f_{wk}^t &= \sum_{j \in K_w} r_{k,j}^t \cdot f_{wj}^{t-1} \\
&= \sum_{\substack{j \neq k \\ j \in K_w}} r_{k,j}^t \cdot f_{wj}^{t-1} + r_{k,k}^t \cdot f_{wj}^{t-1} \\
&= \sum_{\substack{j \neq k \\ j \in K_w}} r_{k,j}^t \cdot f_{wj}^{t-1} + \left[\beta \cdot p_{wk}^t + (1-\beta)\right] \cdot f_{wk}^{t-1} \\
&= \sum_{j \in K_w} \beta \cdot p_{wk}^t \cdot f_{wj}^{t-1} + (1-\beta) \cdot f_{wk}^{t-1} \\
&= \beta \cdot p_{wk}^t \cdot \sum_{j \in K_w} f_{wj}^{t-1} + (1-\beta) \cdot f_{wk}^{t-1},\ \forall k \in K_w,\ \forall w \in W
\end{aligned} \tag{14}$$

Note that $\sum_{j \in K_w} f_j^{t-1} = q_w$, then we can obtain the route flow (Cantarella and Cascetta, 1995):

$$f_{wk}^t = \beta \cdot q_w \cdot p_{wk}^t + (1-\beta) \cdot f_{wk}^{t-1},\ \forall k \in K_w,\ \forall w \in W \tag{15}$$

Generally, the route choice probability p_{wk}^t is calculated in terms of the random utility theory. It is assumed that the error terms of the perceived utilities associated with all paths follow the Gumbel distribution, thus the logit-type function can be adopted here to obtain the route choice probability:

$$p_{wk}^t = \frac{e^{-\theta C_{wk}^t}}{\sum_{j \in K_w} e^{-\theta C_{wj}^t}},\ \forall k \in K_w,\ \forall w \in W \tag{16}$$

where θ is related to the perceived utility standard deviation (SD) by the form of $SD(C_{wk}^t) = \pi/\sqrt{6}\theta$ for all of the days. A large value of θ indicates a small standard deviation, i.e., the perception error is small and travelers will tend to choose the path with minimum cost. When θ approaches infinite, then it becomes deterministic user equilibrium problem. If the value of θ is small, the standard deviation will be large, and the perception error will be large. Thus, travelers will use many different routes and some of them may be much expensive than the shortest path (Sheffi, 1985).

Substituting Eq. (16) into (15) and aggregating it in a vector form, then we can obtain that:

$$\boldsymbol{f}_w^t = \beta \cdot q_w \cdot \boldsymbol{p}(\boldsymbol{C}_w^t) + (1-\beta) \cdot \boldsymbol{f}_w^{t-1} \tag{17}$$

It should be noted that the flow $\boldsymbol{f}_w^t$ in Eq. (17) contains two components (Liu et al., 2017): the one is inertia, which reflects the part of travelers who will insist on the route choices the same as the previous day; and the other is regret, which reflects those travelers who will change to another route different from the previous day. However, we cannot just treat the first term in Eq. (17) as the regret and the second term as the inertia, because the first term indicates the reconsideration portion of travelers, namely, these reconsidered travelers may still insist on the previous route. Actually, the regret and inertia effects are integrated in the cost updating and flow updating models.

The day-to-day dynamics model introduced above is a deterministic process model, which is in line with the classic work of Cantarella and Cascetta (1995). As claimed in Cantarella and Cascetta (1995), the general framework of the deterministic day-to-day dynamics model proposed in their paper can evolve towards many different types of attractors (e.g., fixed-point equilibrium state, periodic equilibrium state, and chaotic state). It should be noted that LPR data collected for the calibration of day-to-day dynamcis model is neither from an equilibration state, nor after a disruption; thus, the general deterministic process model of day-to-day dynamics proposed in Cantarella and Cascetta (1995) is a very suitable alternative for this paper.

It is obvious that in the day-to-day dynamics model, α, β and θ are three parameters to be calibrated. To simplify the notation, in the kriging metamodel introduced in the next section, we group these three parameters in a set and denote it by $\boldsymbol{x} = (\alpha, \beta, \theta)$, and

say $\boldsymbol{x}$ is a set of variables in the kriging metamodel. In the next section, we will introduce how to trace vehicle's trajectory based on the LPR data and how to calibrate and validate the day-to-day dynamics model based on the surrogate-based simulation optimization approach with the vehicle's trajectory data.

3 Methodology

One of the most significant advantages of the LPR data is that we can trace the same vehicle between upstream and downstream intersections with the license plate number and timestamp sequence and then obtain its trajectory. In this section, we propose a surrogate-based simulation optimization approach to calibrate the route-based day-to-day dynamics model with the real-world LPR data.

3.1 Tracing vehicles' trajectories

It is well known that with a given link flow pattern, the corresponding route flow pattern is generally not unique. In order to obtain the unique route flow pattern that occurs in reality, we need to trace the day-to-day vehicles' trajectories, which can be recognized by the LPR cameras from each day. Five types of vehicle records during the procedure of tracing vehicles' trajectories are cast off. Firstly, the recorded vehicles without specific license plate numbers are eliminated, and this will not affect the calibration results because only less than 1% vehicles are recorded without specific license plate numbers, and these eliminated vehicles just like the sampled vehicles, which do not affect the results. Secondly, the recorded vehicles equipped with non-native plates are excluded from the database due to the ineffectiveness for the analysis of the day-to-day dynamics. In this paper, we focus on the analysis of commuters' day-to-day dynamic route choice and route adjustment process, thus the vehicles with non-native plates are mostly non-commuters, which should be eliminated. Thirdly, the buses have fixed routes, therefore they should be eliminated from the database. As for bus transport, the daily route is fixed and would not change with day-to-day dynamic evolutions, thus they are not considered in this paper. However, one might also investigate the day-to-day dynamics model from the perspective of the person (rather than vehicles like this paper), then the public transport users should be taken into consideration because they will change their daily public transport modes and lines dynamically. Fourthly, the trucks are not commuter vehicles, thus should be eliminated.

Finally, the taxis are cruising in the cities without relatively fixed origins and destinations, thus they are not the focus of day-to-day dynamics in this paper. Therefore, the eliminated data will not affect the results of the day-to-day dynamics model in this paper.

After eliminating the vehicle records discussed above, then we can define the *regular travels* as the travels that are recorded at least three times during the morning peak hours (07:00-09:30) for weekdays of one week, and the corresponding vehicles are *regular vehicles*. Compared to other vehicles or nonpeak hours, the day-to-day dynamics of travel trajectories of regular vehicles on the peak hours can be easily traced. The afternoon peak hour is not suitable for the analysis here, because many travelers may not go back home directly after work, but instead have some social activities. The detailed procedures for LPR data processing are summarized as follows:

Algorithm 1. *Procedures for data processing.*

Step 1: Eliminate the recorded vehicles with defective license plate numbers or unrecognized numbers.

Step 2: Eliminate the recorded vehicles equipped with non-native license plates.

Step 3: Eliminate the buses, trucks, and taxis through the color recognition, and only reserve the private vehicles for analysis.

Step 4: Select the regular vehicles and trace their daily route choices based on regular vehicles' trajectories.

Step 5: For each OD pair, aggregate the flows on each route for each day.

It should be noting that the day-to-day dynamics model discussed in this paper focuses on the travelers' route choice and route switching behaviors from one day to the next day, especially on the commuters' travel behaviors with private vehicles. This is in line with the mainstream research in the day-to-day dynamics model. As for public transport, the daily route is fixed and would not change with day-to-day dynamic evolutions, thus they are not considered in this paper. However, one might also investigate the day-to-day dynamics model from the perspective of the person (rather than vehicles like this paper), then the public transport users should be taken into consideration because they will change their daily public transport modes and lines dynamically.

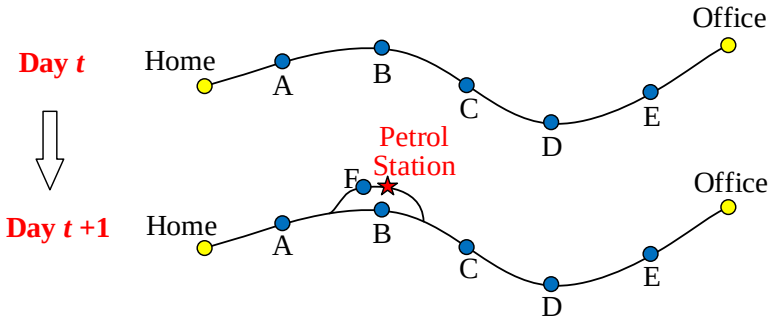

Figure 1: Illustration of the fine-grained route change behaviors

In a real-world transportation network, there may be so many intersections equipped with LPR cameras. This may result in a serious problem for the day-to-day dynamics analysis, i.e., the fine-grained and too specific route plans in the observed day-to-day dynamics evolution process. For example, as shown in Figure 1, a commuter departs from his/her home for the working place, and he/she will go through a series intersections equipped with LPR cameras. On day t, his/her trajectory is traced by the LPR data as Home→A→B→C→D→E→Office. However, on the next day $t+1$, he/she may go to the petrol station near location B, but his/her position is identified by the LPR camera F, rather than B. Thus, the trajectory is recognized as Home→A→F→C→D→E→Office, which is different from the previous day's trajectory. This is similar to the red-blue bus problem or the overlapping problem in the logit-based route choice model. To overcome this fine-grained route change behaviors in the observed day-to-day dynamics evolution process, we make a rational approximation in this paper, i.e., only arterial roads (or expressways) are abstracted in the network for day-to-day dynamics analysis. This approximation avoids the over-frequent fine-grained route changes in the observed day-to-day dynamics evolution process, but still keeps the substantive characteristics of day-to-day dynamics.

3.2 Surrogate-based simulation optimization

The surrogate-based simulation optimization approach is dominant for solving the optimization problems with expensive-to-evaluate response functions. Here we will use the kriging metamodel, which is a typical surrogate-based simulation optimization approach, to calibrate the route based day-to-day dynamics model introduced in Section 2. The detailed process of the calibration is described in the flow diagram of Figure 2.

3.2.1 The original model

It is intuitive to define an objective function for the calibration of day-to-day dynamics with the observed and theoretical traffic flows. Given an initial set of sampled values of the variables $\boldsymbol{x}=(\alpha,\beta,\theta)$ and the initial evolutionary state[2], we can obtain the traffic flows and costs from the evolution process of the day-to-day dynamics model. Compared with the observed traffic flows, we can define the optimization model with the mean square error (MSE) as follows:

$$\begin{aligned}
&\min_{\boldsymbol{x}=(\alpha,\beta,\theta)} \frac{1}{|T|}\cdot\frac{1}{|W|}\sum_{t\in T}\sum_{w\in W}\frac{1}{|K_w|}\sum_{k\in K_w}\left(f_{wk}^{t}-\hat{f}_{wk}^{t}\right)^2 \\
&=\frac{1}{|T|}\cdot\frac{1}{|W|}\sum_{t\in T}\sum_{w\in W}\frac{1}{|K_w|}\sum_{k\in K_w}\left[\left(\beta\cdot p_{wk}^{t}\cdot\sum_{j\in K_w}f_{wj}^{t-1}+(1-\beta)\cdot f_{wk}^{t-1}\right)-\hat{f}_{wk}^{t}\right]^2 \\
&=\frac{1}{|T|}\cdot\frac{1}{|W|}\sum_{t\in T}\sum_{w\in W}\frac{1}{|K_w|}\sum_{k\in K_w}\left[\left(\beta\cdot\frac{e^{-\theta C_{wk}^{t}}}{\sum_{j\in K_w}e^{-\theta C_{wj}^{t}}}\cdot\sum_{j\in K_w}f_{wj}^{t-1}+(1-\beta)\cdot f_{wk}^{t-1}\right)-\hat{f}_{wk}^{t}\right]^2
\end{aligned} \tag{18}$$

where (i) f_{wk}^{t} and $\hat{f}_{wk}^{t}$ are the theoretical and observed route flow of route $k\in K_w$ between OD pair $w\in W$ on day $t\in T$, respectively, (ii) $|T|$, $|W|$ and $|K_w|$ are the cardinalities of the set of epochs, the set of OD pairs, and the set of routes between OD pair $w\in W$, respectively, and (iii) the forecasted cost C_{wk}^{t} is defined as:

$$C_{wk}^{t}=\alpha c_{wk}^{t-1}+(1-\alpha)C_{wk}^{t-1} \tag{19}$$

where c_{wk}^{t-1} and C_{wk}^{t-1} are the actual the forecasted costs of route k between OD pair $w\in W$ on day $t-1$.

[2] The initial evolutionary state of the flows can be set as any feasible flows. However, a good initial state, which better reflects the actual traffic situations, can accelerate the computational speed to reach a relatively stationary state. Therefore, we set the initial flows the same as the observed flows with LPR data.

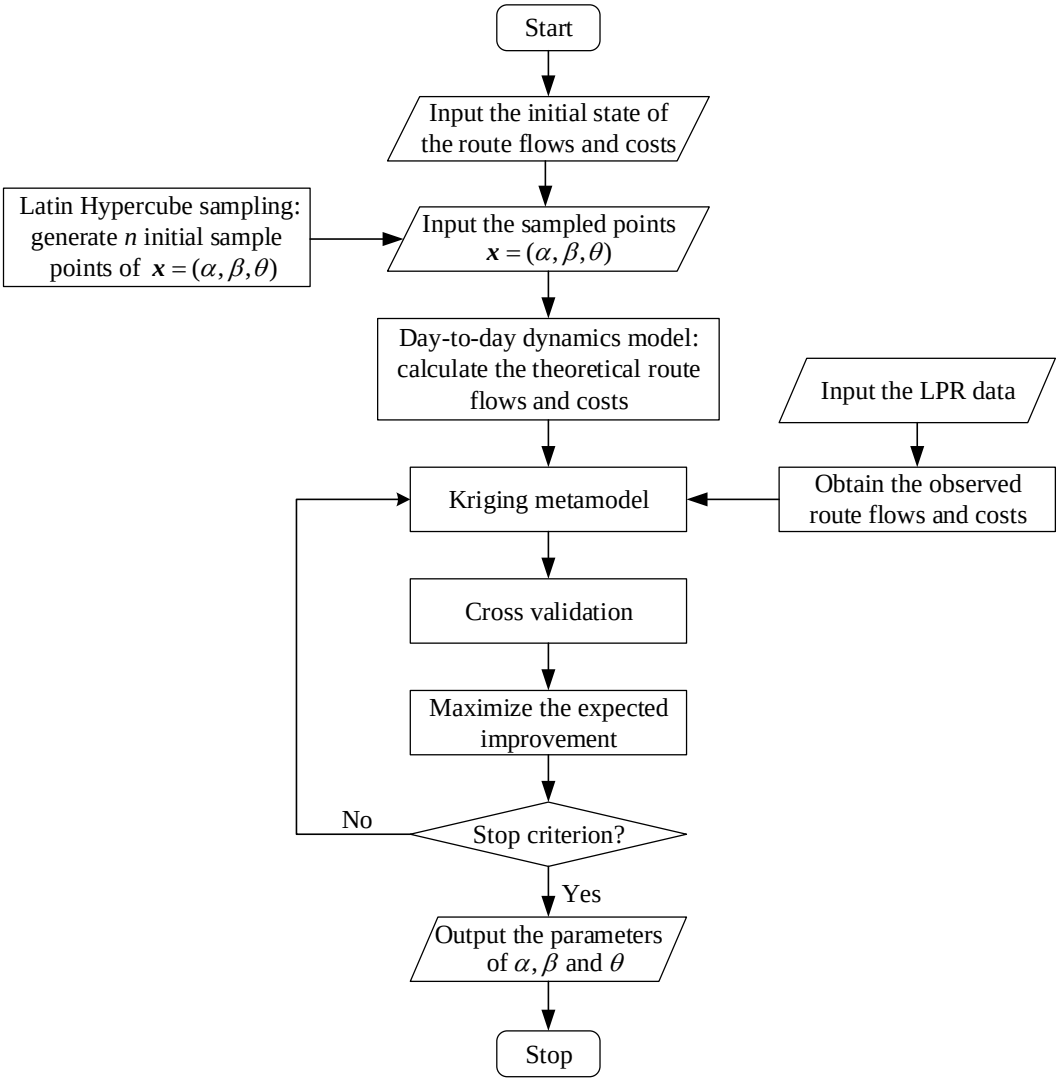

Figure 2: Flowchart of the calibration for the day-to-day dynamics model

Therefore, it can be seen that the response function (18) is a highly nonlinear and complex one of the variables $\boldsymbol{x}=(\alpha,\beta,\theta)$. To illustrate the complexity of this multi-modal response function (18), we depict the surface of the response function in Figure 3, when θ is set as 1.0 and α and β take different combinations of values between 0 and 1. Note that the other input data are same as those used in the case study in Section 4.

From Figure 3, it is obvious that the optimization model (18) is highly nonlinear and multi-modal, and thus it is very challenging to calibrate the variables of $\boldsymbol{x}=(\alpha,\beta,\theta)$. When we calculate the objective function for a particular input variable, we need to first obtain the traffic flows and costs from the first day to the last day in terms of the flow and cost updating processes in Eqs. (6) and (17) without a closed-form function, which is a tedious work especially when the network size is large-scale and the period is long-term. Therefore, gradient-

based nonlinear regression algorithms or other analytical optimization approaches are not applicative for solving the optimization model defined in (18). Here, it is reasonable to adopt a surrogate-based simulation optimization approach to deal with the expensive-to-evaluate objective function, which will be introduced in following sections.

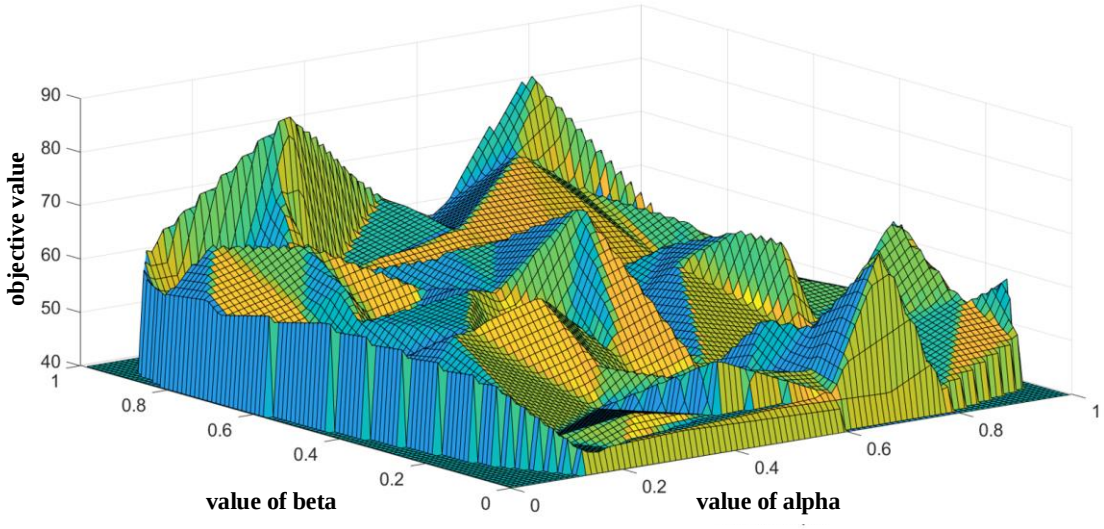

Figure 3: Illustration of the highly nonlinear and multi-modal response function ($\theta = 1.0$)

3.2.2 A surrogate model: the Kriging metamodel

The kriging metamodel of the simulation-based optimization is used as a surrogate in this paper to calibrate the parameters of α, β and θ in the day-to-day dynamics model. In this kriging metamodel, the optimization model defined in (18) is replaced by the sum of a constant value and a Gaussian random error term as follows[3]:

$$Y(\boldsymbol{x}) = \mu + y(\boldsymbol{x}) \tag{20}$$

where $Y(\boldsymbol{x})$ is the response function (i.e., the MSE defined in (18)), μ is the mean of $Y(\boldsymbol{x})$, and $y(\boldsymbol{x})$ is a stationary Gaussian random process with the mean $\mathrm{E}[y(\boldsymbol{x})] = 0$, variance σ^2 and non-zero covariance. The covariance is defined as follows:

$$\mathrm{Cov}[y(\boldsymbol{x}^{(u)}), y(\boldsymbol{x}^{(v)})] = \sigma^2 \cdot \psi(\boldsymbol{x}^{(u)}, \boldsymbol{x}^{(v)}) \tag{21}$$

where $\mathrm{Cov}[y(\boldsymbol{x}^{(u)}), y(\boldsymbol{x}^{(v)})]$ is the covariance between two arbitrary points $\boldsymbol{x}^{(u)}$ and $\boldsymbol{x}^{(v)}$ and $\psi(\boldsymbol{x}^{(u)}, \boldsymbol{x}^{(v)})$ is the kriging function (also called the Gaussian exponential correlation

[3] Actually, this is a stochastic process model in essences. In the stochastic process approach, the errors are correlated relating to the distances (not Euclidean distance, but a function of Euclidean distance) between sampled points, rather than independent in deterministic process model. After introducing the correlated error terms, it is powerful to replace the regression terms in deterministic process model by a simple constant term, resulting in a stochastic process model as shown in Eq. (20). The detailed analysis is referred to Jones et al. (1998).

function). The kriging function is defined by a function of the Euclidean distance between $\boldsymbol{x}^{(u)}$ and $\boldsymbol{x}^{(v)}$ as follows:

$$\psi(\boldsymbol{x}^{(u)}, \boldsymbol{x}^{(v)}) = \exp\left[-\sum_{l=1}^{L} \lambda_l \left(x_l^{(u)} - x_l^{(v)} \right)^2 \right] \tag{22}$$

where $\boldsymbol{\lambda} = [\lambda_1, \cdots, \lambda_l, \cdots, \lambda_L]$ denotes the vector of scaling coefficients of the unknown model parameters to be tuned, $x_l^{(u)}$ and $x_l^{(v)}$ denote the lth variable in $\boldsymbol{x}^{(u)}$ and $\boldsymbol{x}^{(v)}$, and L denotes the dimension of $\boldsymbol{x}$ (here $L = 3$ in the day-to-day dynamics model in this paper). Note that the parameter λ_l can be regarded as measuring the importance of the variable x_l, saying that the variable x_l is important means that even a small value of $\left| x_l^{(u)} - x_l^{(v)} \right|$ may resulting in a significant difference in the response function at $\boldsymbol{x}^{(u)}$ and $\boldsymbol{x}^{(v)}$. Thus, the larger of λ_l, and the greater of the 'distance' between $x_l^{(u)}$ and $x_l^{(v)}$, hence the lower of correlation between them.

Now the kriging metamodel has five parameters to be estimated: μ, σ^2, λ_1 for α, λ_2 for β and λ_3 for θ. From the derivation by Sacks et al. (1989) and Jones et al. (1998), with n input variables of $\boldsymbol{x} = (\alpha, \beta, \theta)$, we can estimate these five parameters through maximizing the likelihood as follows:

$$\max_{\mu, \sigma^2, \boldsymbol{\lambda}} \frac{1}{(2\pi\sigma^2)^{n/2} \sqrt{|\boldsymbol{\Psi}|}} \exp\left[-\frac{(\boldsymbol{y} - \boldsymbol{1}\mu)^T \boldsymbol{\Psi}^{-1} (\boldsymbol{y} - \boldsymbol{1}\mu)}{2\sigma^2} \right] \tag{23}$$

where $\boldsymbol{y}$ is the observed MSE defined in (18), $\boldsymbol{1}$ is the $n \times 1$ unit column, and n is the number of sample points for variable $\boldsymbol{x} = (\alpha, \beta, \theta)$, which will be determined by the design of experiment. $|\boldsymbol{\Psi}|$ is the determinant of $\boldsymbol{\Psi}$, where $\boldsymbol{\Psi}$ is the matrix of $\psi(\boldsymbol{x}, \boldsymbol{x}')$ defined as follows:

$$\boldsymbol{\Psi} = \begin{pmatrix} \psi(\boldsymbol{x}^{(1)}, \boldsymbol{x}^{(1)}) & \psi(\boldsymbol{x}^{(1)}, \boldsymbol{x}^{(2)}) & \cdots & \psi(\boldsymbol{x}^{(1)}, \boldsymbol{x}^{(n)}) \\ \psi(\boldsymbol{x}^{(2)}, \boldsymbol{x}^{(1)}) & \psi(\boldsymbol{x}^{(2)}, \boldsymbol{x}^{(2)}) & \cdots & \psi(\boldsymbol{x}^{(2)}, \boldsymbol{x}^{(n)}) \\ \vdots & \vdots & \ddots & \vdots \\ \psi(\boldsymbol{x}^{(n)}, \boldsymbol{x}^{(1)}) & \psi(\boldsymbol{x}^{(n)}, \boldsymbol{x}^{(2)}) & \cdots & \psi(\boldsymbol{x}^{(n)}, \boldsymbol{x}^{(n)}) \end{pmatrix} \in \mathbb{R}^{n \times n} \tag{24}$$

The maximization of the likelihood function defined in (23) can be approximated with the natural logarithm and neglecting the constant term, thus giving a concise log-likelihood

function as follows:

$$-\frac{n}{2}\ln(\sigma^2)-\frac{1}{2}\ln\left(\left|\boldsymbol{\Psi}\right|\right)-\frac{(\boldsymbol{y}-\boldsymbol{1}\mu)^{\mathrm{T}}\boldsymbol{\Psi}^{-1}(\boldsymbol{y}-\boldsymbol{1}\mu)}{2\sigma^2}+\text{constant} \tag{25}$$

Solving the first derivations of the above log-likelihood function and setting them to be zero, then we can obtain the estimation of μ, σ^2, λ_1, λ_2 and λ_3. However, as claimed in Kleijnen (2015), this estimation is a difficult mathematical problem, and the divide-and-conquer methodology (e.g., profile likelihood or concentrated likelihood method) is used here for estimation. The algorithm to estimate the above five parameters is summarized as follows:

Algorithm 2. *Procedure for parameters estimation.*

Step 1: Initialize the parameters of $\hat{\lambda}_1$, $\hat{\lambda}_2$ and $\hat{\lambda}_3$, and obtain the $\psi(\boldsymbol{x}^{(u)},\boldsymbol{x}^{(v)})$ defined in Eq. (22) and $\hat{\boldsymbol{\Psi}}$ defined in Eq. (24).

Step 2: Solve the first derivation of (25) with respect to μ, which gives the estimator of the mean:

$$\hat{\mu}=\frac{\boldsymbol{1}^{\mathrm{T}}\hat{\boldsymbol{\Psi}}^{-1}\boldsymbol{y}}{\boldsymbol{1}^{\mathrm{T}}\hat{\boldsymbol{\Psi}}^{-1}\boldsymbol{1}} \tag{26}$$

Step 3: Substitute $\hat{\boldsymbol{\Psi}}$ obtained in *Step 1* and $\hat{\mu}$ obtained in *Step 2* into (25), and solve its first derivation with respect to σ^2, which gives the estimator of the variance:

$$\hat{\sigma}^2=\frac{(\boldsymbol{y}-\boldsymbol{1}\hat{\mu})^{\mathrm{T}}\hat{\boldsymbol{\Psi}}^{-1}(\boldsymbol{y}-\boldsymbol{1}\hat{\mu})}{n} \tag{27}$$

Step 4: Substitute $\hat{\mu}$ and $\hat{\sigma}^2$ into (25), and then it is only the function of λ_1, λ_2 and λ_3. Solve the remaining problem (Kleijnen, 2015; Lophaven et al., 2002):

$$\min\ \hat{\sigma}^2\left|\hat{\boldsymbol{\Psi}}\right|^{-n} \tag{28}$$

and then update $\hat{\lambda}_1$, $\hat{\lambda}_2$ and $\hat{\lambda}_3$.

Step 5: Update $\hat{\psi}$ and $\hat{\boldsymbol{\Psi}}$ with the updated $\hat{\lambda}_1$, $\hat{\lambda}_2$ and $\hat{\lambda}_3$, and substitute this updated $\hat{\boldsymbol{\Psi}}$ into Eqs. (26) and (27).

Step 6: If the convergence criteria have not been satisfied, then return to Step 2; otherwise, stop and output the estimators of $\hat{\mu}$, $\hat{\sigma}^2$, $\hat{\lambda}_1$, $\hat{\lambda}_2$ and $\hat{\lambda}_3$.

Up to now, the maximum likelihood estimate of the response function $Y(\boldsymbol{x})$ can be obtained by the following function:

$$\hat{Y}(\boldsymbol{x}) = \hat{\mu} + \hat{\boldsymbol{\psi}}^{\mathrm{T}}\hat{\boldsymbol{\Psi}}^{-1}(\boldsymbol{y} - \boldsymbol{1}\hat{\mu}) \tag{29}$$

where $\hat{Y}(\boldsymbol{x})$ is the estimate of the response function of $Y(\boldsymbol{x})$, and $\hat{\boldsymbol{\psi}}$ is the estimate of the correlation vector between the ith sample point $x^{(i)}$ and the untried point $\boldsymbol{X}$, which is defined as follows:

$$\hat{\boldsymbol{\psi}} = \begin{pmatrix} \hat{\psi}(\boldsymbol{x}^{(1)}, \boldsymbol{x}) \\ \hat{\psi}(\boldsymbol{x}^{(2)}, \boldsymbol{x}) \\ \vdots \\ \hat{\psi}(\boldsymbol{x}^{(n)}, \boldsymbol{x}) \end{pmatrix} \tag{30}$$

That is to say, when we have a new input variable $\boldsymbol{X}$, then we can first obtain the correlation vector based on (30), and then obtain its response in terms of (29). Note that the errors induced by the correlation will also influence the estimation of prediction accuracy. The estimation error now is of the form as follows:

$$\hat{s}^2(\boldsymbol{x}) = \hat{\sigma}^2 \cdot \left[1 - \hat{\boldsymbol{\psi}}^{\mathrm{T}}\hat{\boldsymbol{\Psi}}^{-1}\hat{\boldsymbol{\psi}} + \frac{\left(1 - \boldsymbol{1}^{\mathrm{T}}\hat{\boldsymbol{\Psi}}^{-1}\hat{\boldsymbol{\psi}}\right)^2}{\boldsymbol{1}^{\mathrm{T}}\hat{\boldsymbol{\Psi}}^{-1}\hat{\boldsymbol{\psi}}} \right] \tag{31}$$

With the kriging metamodel introduced above, then we can obtain the estimated optimal values for the variables $\boldsymbol{x} = (\alpha, \beta, \theta)$ with the maximization of expected improvement discussed in Section 3.2.5.

3.2.3 Design of experiment

In the kriging metamodel, we need to generate n initial sample points of $\boldsymbol{X}$, and this process is called the 'space-filling' design of experiment (DoE). DoE affects the solution quality and the computational efficiency, and a better DoE strategy will make it find a better solution within less computation time. The Monte Carlo sampling technique is one of the most widely used sampling approaches using random or pseudo-random numbers to sample from a probability distribution. It is entirely random in principle, thus with enough iterations, it will recreate the same distribution as the original objective function through sampling. However, the problem of 'clustering' may be encountered when only a small number of sample points are afforded for simulation (e.g., see p. 457 in Palisade Corporation, 2004).

To overcome the 'clustering' problem in the Monte Carlo sampling, McKay et al. (1979) introduced Latin Hypercube sampling technique in the DoE. Different from the entirely random Monte Carlo sampling, Latin Hypercube sampling stratifies the input probability distributions

to ensure each of the input variable has all portions of its range represented (Sacks et al., 1989). Iman and Helton (1988) compared the Latin Hypercube sampling with Monte Carlo sampling and showed a significant advantage of the Latin Hypercube sampling in the DoE. In this paper, we use the Latin Hypercube sampling technique to generate the initial sample points for the kriging metamodel. More specifically, each variable of $\boldsymbol{x}$ is stratified into n equal intervals (n is the number of desired sample points), and in each subinterval, a sample point is randomly generated. When the afforded number of simulation n is modest, this Latin Hypercube sampling approach makes simulations converge faster than Monte Carlo sampling method.

3.2.4 Cross validation

Substituting the initial sampled points generated by the Latin Hypercube sampling approach into the kriging metamodel, then we can obtain an initial estimation of the response function in (29). In addition, we use the cross validation to evaluate the accuracy of the model. The basic idea behind the cross validation is to leave out one of the sampled points, called $\boldsymbol{x}^{(i)}$, and then predict its response value back with the only $n-1$ remaining points. We can also get the cross-validated standard error without the sampling point $\boldsymbol{x}^{(i)}$ based on the Eq. (31). Then the standardized cross-validated residual (SCVR) is defined as follows:

$$\mathrm{SCVR} = \frac{Y(\boldsymbol{x}^{(i)}) - Y_{-i}(\boldsymbol{x}^{(i)})}{s_{-i}(\boldsymbol{x}^{(i)})} \tag{32}$$

where $Y(\boldsymbol{x}^{(i)})$ is the observed response value of sampled point $\boldsymbol{x}^{(i)}$, $Y_{-i}(\boldsymbol{x}^{(i)})$ is the predicted value with the cross validation leaving out the sampled point $\boldsymbol{x}^{(i)}$, and $s_{-i}(\boldsymbol{x}^{(i)})$ is the cross-validated standard error without the sampling point $\boldsymbol{x}^{(i)}$. It is said that a metamodel is valid when the value of SCVR is roughly in the interval $[-3,+3]$, which is a 99.7% confidence interval in statistics. However, sometimes the value of SCVR may be out of the interval $[-3,+3]$, thus some transformations are necessary to improve the fit of the metamodel. The log-transformation and the inverse-transformation are two typical transformation methods. We will test these two transformations when the value of SCVR is out of the interval $[-3,+3]$.

3.2.5 An efficient method to get an approximation solution for expected improvement (EI) maximization

Up to now, the optimal solution solved by the kriging metamodel may be a local optimum because it neglects the uncertainty in the response function (Jones et al., 1998). In order to obtain an efficient global approximation, here we use the concept of expected improvement (EI) and seek for a maximization of EI to reach the global approximation. Specifically, EI maximization is an infill criterion to generate new sample points, and next we will introduce how to maximize the EI.

As for the n sampled points of $\boldsymbol{x}$, we can obtain n values of $Y^{(n)}$ in terms of (29). Define the current best value of the response function as $Y_{\min} = \min(Y^{(1)}, \cdots, Y^{(n)})$. For an untried point $\boldsymbol{x}$, we model its response through a normally distributed random variable Y with mean $\hat{Y}$ in Eq. (29) and variance $\hat{s}^2$ in Eq. (31). Then the expected improvement at point $\boldsymbol{x}$ is expressed as follows:

$$\mathrm{E}[I(\boldsymbol{x})] \equiv \mathrm{E}[\max(Y_{\min} - Y), 0] \tag{33}$$

where $I(\boldsymbol{x}) = \max(Y_{\min} - Y, 0)$ is the improvement at point $\boldsymbol{x}$, and $\mathrm{E}[I(\boldsymbol{x})]$ is the EI at point $\boldsymbol{x}$. Due to the normal distribution of Y, the closed-form of $\mathrm{E}[I(\boldsymbol{x})]$ can be expressed as follows:

$$\mathrm{E}[I(\boldsymbol{x})] = \begin{cases} (Y_{\min} - \hat{Y})\Phi\left(\dfrac{Y_{\min} - \hat{Y}}{\hat{s}}\right) + \hat{s}\phi\left(\dfrac{Y_{\min} - \hat{Y}}{\hat{s}}\right) & \text{if } \hat{s} > 0 \\ 0 & \text{if } \hat{s} = 0 \end{cases} \tag{34}$$

where $\Phi(\cdot)$ and $\phi(\cdot)$ are the standard normal density and distribution functions, respectively. Therefore, the EI function can be easily computed with an analytical solution under the Gaussian assumptions and the optimum now is an efficient global approximation value.

Compared to other heuristic algorithms, such as the genetic algorithms and neural network algorithms, the surrogate-based simulation optimization method can obtain reliable outputs without running the expensive-to-evaluate objective function. Therefore, it takes less computation time and cost. Besides, with the process of expected improvement (EI) maximization (Jones et al., 1998), we can obtain an efficient global approximation of the solution because the closed-form of the EI function can be derived and easily computed.

Therefore, we choose the surrogate-based simulation optimization method rather than some heuristic algorithms, e.g., the genetic algorithm and the neural network, to calibrate the parameters in the day-to-day dynamics model.

4 Case Study

4.1 Study area and LPR data analysis

To demonstrate the effectiveness of the methodology proposed in this paper, a case study is conducted in this section. The study area is located in the downtown area in Yuyao City, China. This area consists of 31 LPR detect points in 40km^2 as shown in Figure 4. The LPR data provided is from June 15, 2018 to July 3, 2018. The total number of records of regular vehicles defined in Section 3.1 reaches up to 7,588,041 during the study period of 19 days inside the study area. An illustration of the LPR data label is provided in Table 2. The case study is coded in Python 3.5 running on a desktop with Intel(R) Core(TM) i5-8400 CPU @ 2.80 Hz, 81 GHz and 8.00G RAM.

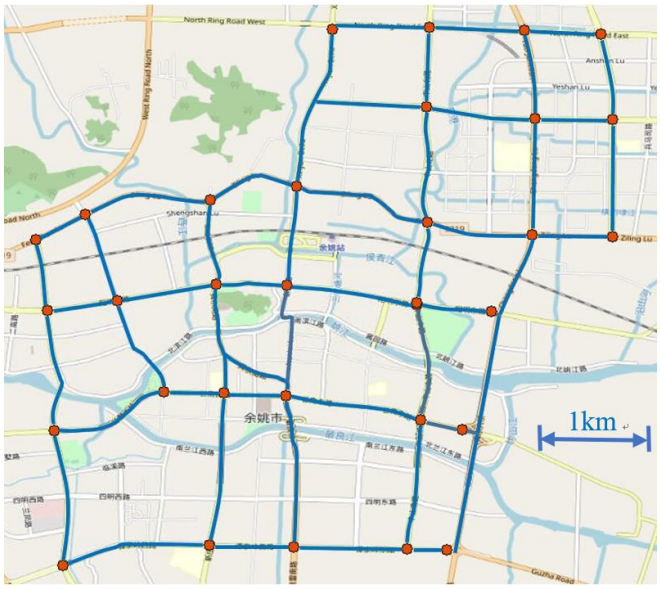

Figure 4: Study area and LPR locations (red points: LPR locations, blue lines: road links)

Table 2: Illustration of the LPR data

License Plate No.	Timestamp	Intersection No.	Intersection Name	Lane No.	Speed	Entrance Direction
ZB 1234[4]	2018-06-26 07:43:40	330281000 000010356	Intersection of Zhongshan Road and Xianqindi Road	02	40	3

[4] The capital letter 'Z', which is originally written in Chinese, indicates Zhejiang Province in China.

Notes:

1) The license plate number in Yuyao City starts from ‘ZB’ followed by four number or capital letters.

2) The timestamp recorded the date and time with the precision of 1 second.

3) The intersection number is made up of 18 numbers.

4) The intersection number and name also distinguish the LPR points.

5) The lane number begins with ‘01’ from the outside to the inside.

6) The recorded speed is positive integers (km/h).

7) As for the entrance direction, ‘01’ represents the north, ‘02’ represents the east, ‘03’ represents the south, and ‘04’ represents the west.

Note that the traffic demand flows are not input data, but they can be computed through the LPR data by aggregating the same origin and destination inside the study area. The actual route costs on a particular day can be measured by averaging the route costs of all vehicles on the same day, and each vehicle’s cost can be obtained by the recorded timestamp at its origin and destination. In this paper, we use the BPR (Bureau of Public Roads) function to calculate the forecasted link travel costs, and then add the link costs belong to the same route as the forecasted route costs. Our focus in this manuscript is on the day-to-day dynamic route choice and route adjustment behavior. For a particular day, we treat is a static traffic flow model; thus congestion is not taken into consideration. In the future work, we will extend it to a doubly dynamics model, which incorporates the within-day dynamics model (e.g., cell/link transmission model) and the day-to-day dynamics model to better describe the system dynamics.

4.2 Results

Although travelers’ route choice behaviors evolve from day to day, the real route choices may not be the whole feasible route set physically. Actually, most of the travelers may have a psychological route set, which is much smaller than the physical route set. As shown in Figure 5, during the study period, almost 80% of the travelers choose no more than 3 different routes as their daily routes. This is intuitive with our daily life. Imagining that in a real-world travel, one from his/her home to his/her work place from day to day, he/she may only choose the most frequently used route, and if this route is over-saturated or he/she has some special tasks in

some day, he/she may choose other alternative routes. However, the number of alternative routes must be much smaller than the feasible routes between his/her home and work place, due to the high costs of the alternative routes.

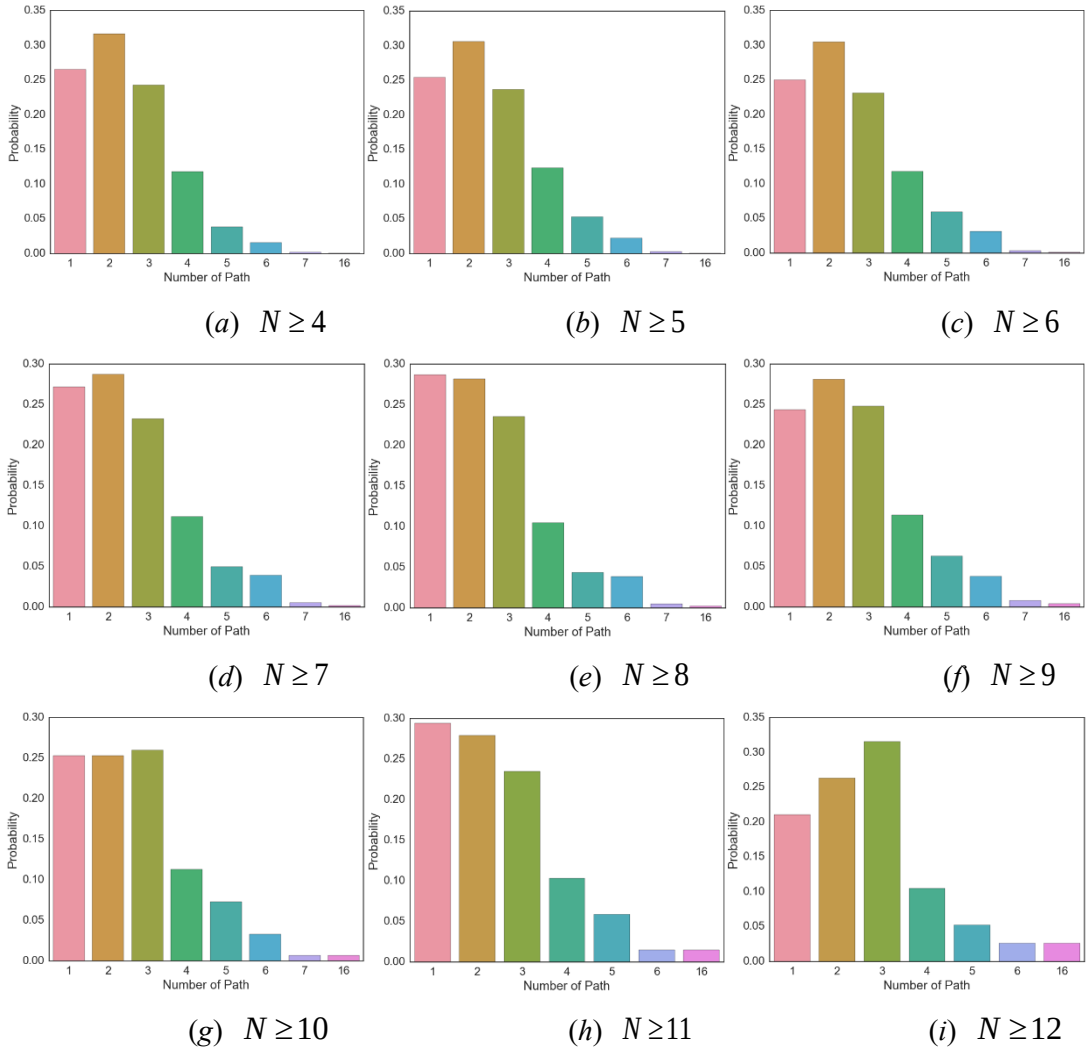

Figure 5: Number of routes chosen by travelers from day to day (N is the smallest number of days that a traveler occurs inside the study area equipped with LPR cameras during the study period)

With the proposed methodology of calibrating the day-to-day dynamics model and the LPR data obtained in Yuyao City, the parameters are finally calibrated as $\alpha = 0.43$, $\beta = 0.51$ and $\theta = 3.56$. It reveals that when travelers forecast the travel costs for the next day, the actual costs of the current day only weight 43%, while the weight of the forecasted travel costs of the current day reaches up to 57%. Similarly, more than half travelers will reconsider the travel routes in the next day and make decisions whether to change to other routes or not, based on

the logit-type utility function, while 49% travelers would not make any reconsiderations. There are no specific criteria for evaluation of the calibrated value of α. Cantarella and Cascetta (1995) stated that $\alpha \in [0.4, 0.8]$ seems likely and our result is still in this region. Besides, the parameters of the cost function in a within-day scale do not consider traffic dynamics in this paper but only use the BRP function. In future work, we will integrate the within-day dynamics model and the day-to-day dynamics model to better reflect the traffic dynamics within one day scale.

The parameter θ is a measure of the travelers' sensitivity to the route costs. It is not dimensionless, its unit should be proportional to the reciprocal of the standard deviation of route cost. A large value of θ indicates a small standard deviation, i.e., the perception error is small and travelers will tend to choose the path with minimum cost. When θ approaches infinite, then it becomes deterministic user equilibrium problem. If the value of θ is small, the standard deviation will be large, and the perception error will be large. Thus, travelers will use many different routes and some of them may be much expensive than the shortest path (Sheffi, 1985). The calibrated value of perception variance is $\theta = 3.56$ in this study, which is much larger than that in some SUE models (e.g., Damberg et al., 1996), revealing that the actual psychological route set for the day-to-day dynamics is much smaller than feasible route set physically. The value $\theta = 3.56$ also indicates that the variance of perceived travel costs on different routes among the entire period is $\mathrm{var}(C_{wk}^t) = \pi^2/6\theta^2 = 0.13$, i.e., the error term in the perceived route cost is Gumbel distributed with zero mean and 0.13 of variance.

There are various studies working on the calibration of random utility theory, including Cascetta et al. (1996) for the modified logit route choice model, Cascetta and Papola (2001) for the implicit availability/perception logit-type model, Cascetta et al. (2002) for the logit-type route perception model, and Cantarella and de Luca (2005) for the multilayer feedforward networks of route choice model, just to name a few. It is worth noting that the parameter θ in this paper should be considered included in the cost attribute coefficient to be calibrated against real data, as always the case in a linear utility specification for a random utility model, see Cascetta (2009).

The route flow evolution process is described in Figure 6. It is obvious that the system is not in a stationary state at the end of the study period due to the perturbation of the network and

the limited data that are available. However, this does not influence the calibration framework proposed in this paper. It should be noted that the network system in this study evolves neither from an equilibration state, nor after a disruption. It evolves from a general day, i.e. day *n* in the evolutionary process. With such an input, the system can represent a general day-to-day dynamics process. The convergence trend of the expected improvement is shown in Figure 7. It can be found that the proposed surrogate-based simulation optimization approach for day-to-day dynamics calibration can converge within 8 iterations in this case study.

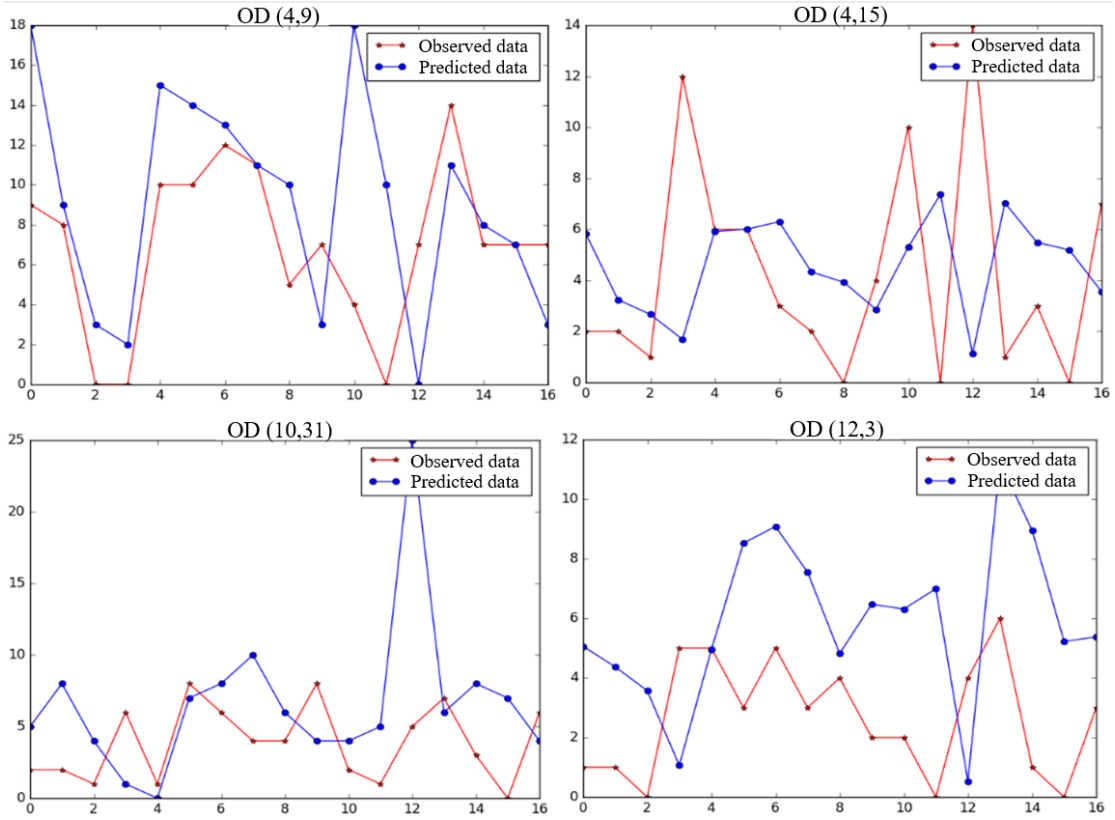

Figure 6: Route flow evolution process from day to day (red lines with asterisk are observed values while blue lines with dot are predicted values)

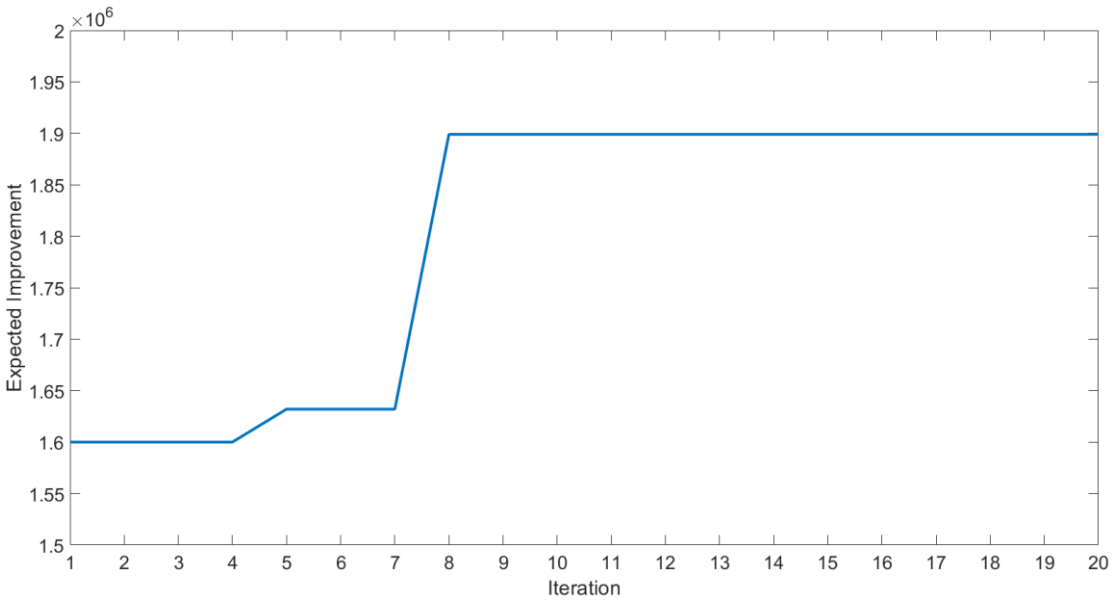

Figure 7: The iteration process of the expected improvement

There are three reasons that the surrogate-based approach takes effect on the calibration of the day-to-day dynamics model. Firstly, it uses the kriging metamodel with the sum of a constant value and a Gaussian random error term, i.e., $Y(\boldsymbol{x}) = \mu + y(\boldsymbol{x})$, to replace the original complicated optimization model defined in Eq. (18). Thus, there is no need to calculate the expensive-to-evaluate function and the computational effort is reduced. Secondly, in the design of experiment procedure, the Latin Hypercube sampling technique is used to generate the initial sample points for the kriging metamodel, and this enables us to find a better solution for space filling within less computation time. Finally, after introducing the expected improvement (EI) maximization procedure, we can obtain an efficient global approximation of the solution because the closed-form of the EI function can be derived and easily computed. Therefore, we choose the surrogate-based simulation optimization method rather than some heuristic algorithms, e.g., the genetic algorithm and the neural network, to calibrate the parameters in the day-to-day dynamics model.

5 Conclusions

This paper studies the day-to-day dynamics model from the perspective of travelers' actual route choice behaviors, and calibrates and validates the route-based day-to-day dynamics model with the real-world LPR data. A surrogate-based simulation optimization approach is proposed to deal with the highly nonlinear and multi-modal response function in the day-to-day dynamics

calibration work. Results reveal that over 70% travelers choose their daily routes no more than 4 different routes. The route cost updating parameter of α, the reconsideration rate of β, and the parameter of θ in the logit-type utility function are calibrated as 0.43, 0.51 and 3.56. When travelers forecast the travel costs for the next day, the actual costs of the current day only weigh 43%, while the weight of the forecasted travel costs of the current day reaches up to 57%. In addition, more than half travelers will reconsider the travel routes in the next day and make decisions whether to change to other routes or not, based on the logit-type utility function, while 49% travelers would not make any reconsiderations. The value $\theta = 3.56$ indicates that the variance of perceived travel costs on different routes among the entire period is $\mathrm{var}(C_{wk}^t) = \pi^2/6\theta^2 = 0.13$, i.e., the error term in the perceived route cost is Gumbel distributed with zero mean and 0.13 of variance. This also indicates that the actual psychological route set for the day-to-day dynamics is much smaller than feasible route set physically.

In this paper, the parameters of α, β and θ are all constant for the whole study period. However, the cost updating ratio and the reconsideration rate may be day-dependent or cost-dependent. For example, the situation may be that the bigger of the gap between the actual cost of the current day and the forecasted cost of the next day, the larger of reconsideration rate for the next day. The day-to-day dynamics model formulation and calibration for the multi-modal transportation systems (e.g., Fu and Lam, 2018; Pi et al., 2019; Zhang and Liu, 2019) with different data sources (e.g., Gu et al., 2019; Xu et al., 2018), need to be further studied in the future research. Some emerging machine/deep learning approaches (e.g., Li et al., 2018; Liu et al., 2019) also can be tested for the calibration of day-to-day dynamics models. With the calibrated parameters in the day-to-day dynamics models, there will be many applications in the transportation management and control, such as Liu et al. (2017), Cheng et al. (2019) and Pan et al. (2019).

Acknowledgement

This study is supported by the General Projects (No. 71771050), the Key Projects (No. 51638004) of the National Natural Science Foundation of China, and the Scientific Research Foundation of Graduate School of Southeast University (No. YBPY1885).

References

Avineri, E., Prashker, J.N., 2005. Sensitivity to travel time variability: travelers' learning perspective. Transp. Res. Part C 13(2), 157-183.

Barton, R.R., Meckesheimer, M., 2006. Metamodel-based simulation optimization, in: Henderson, S.G., Nelson, B.L. (Eds.), Handbook in OR & MS, Vol. 13. Elsevier B.V., pp. 535–574.

Ben-Elia, E., Di Pace, R., Bifulco, G.N., Shiftan, Y., 2013. The impact of travel information's accuracy on route-choice. Transp. Res. Part C 26, 146-159.

Bie, J., Lo, H.K., 2010. Stability and attraction domains of traffic equilibria in a day-to-day dynamical system formulation. Transp. Res. Part B 44(1), 90-107.

Cantarella, G.E., 2013. Day-to-day dynamic models for Intelligent Transportation Systems design and appraisal. Transp. Res. Part C 29, 117–130.

Cantarella, G.E., Cascetta, E., 1995. Dynamic processes and equilibrium in transportation networks: towards a unifying theory. Transp. Sci. 29(4), 305-329.

Cantarella, G.E., de Luca, S., 2005. Multilayer feedforward networks for transportation mode choice analysis: an analysis and a comparison with random utility models. Transp. Res. Part C 13(2), 121-155.

Cantarella, G.E., Velonà, P., Watling, D.P., 2015. Day-to-day dynamics & equilibrium stability in a two-mode transport system with responsive bus operator strategies. Networks Spat. Econ. 15, 485–506.

Cantarella, G.E., Watling, D.P., 2016. A general stochastic process for day-to-day dynamic traffic assignment : formulation , asymptotic behaviour , and stability analysis. Transp. Res. Part B 92, 3–21.

Cardin, M.A., Deng, Y., Sun, C., 2017. Real options and flexibility analysis in design and management of one-way mobility on-demand systems using decision rules. Transp. Res. Part C 84, 265–287.

Cascetta, E., 1987. Static and dynamic models of stochastic assignment to transportation networks. In *Flow control of congested networks* (pp. 91-111). Springer, Berlin, Heidelberg.

Cascetta, E., 1989. A stochastic process approach to the analysis of temporal dynamics in

transportation networks. Transp. Res. Part B 23(1), 1-17.

Cascetta, E., 2009. Transportation Systems Analysis, Springer Science Business Media.

Cascetta, E., Cantarella, G.E., 1991. A day-to-day and within-day dynamic stochastic assignment model. Transp. Res. Part A 25(5), 277-291.

Cascetta, E., Nuzzolo, A., Russo, F., Vitetta, A.,1996. A modified logit route choice model overcoming path overlapping problems: Specification and some calibration results for interurban networks. In *Proceedings of The 13th International Symposium on Transportation and Traffic Theory, Lyon, France, 24-26 July 1996*.

Cascetta, E., Papola, A., 2001. Random utility models with implicit availability/perception of choice alternatives for the simulation of travel demand. Transp. Res. Part C 9(4), 249-263.

Cascetta, E., Russo, F., Viola, F. A., Vitetta, A., 2002. A model of route perception in urban road networks. Transp. Res. Part B 36(7), 577-592.

Chen, D. 2017. Research on traffic flow prediction in the big data environment based on the improved RBF neural network. IEEE T. Ind. Inform. 13(4), 2000-2008.

Chen, X., Xiong, C., He, X., Zhu, Z., Zhang, L., 2016. Time-of-day vehicle mileage fees for congestion mitigation and revenue generation: A simulation-based optimization method and its real-world application. Transp. Res. Part C 63, 71-95.

Cheng, Q., Liu, Z., Szeto, W.Y., 2019. A cell-based dynamic congestion pricing scheme considering travel distance and time delay. Transportmetrica B 7(1), 1286-1304.

Cho, H.J., Hwang, M.C., 2005. Day-to-day vehicular flow dynamics in intelligent transportation network. Math. Comput. Modell. 41(4-5), 501-522.

Chong, L., Osorio, C., 2015. A simulation-based optimization algorithm for dynamic large-scale urban transportation problems. Transp. Sci. 49, 623-636.

Cressie, N., 1990. The origins of kriging. Math. Geol. 22, 239-252.

Damberg, O., Lundgren, J.T., Patriksson, M., 1996. An algorithm for the stochastic user equilibrium problem. Transp. Res. Part B 30(2), 115-131.

Davis, G. A., Nihan, N. L., 1993. Large population approximations of a general stochastic traffic assignment model. Oper. Res. 41(1), 169-178.

Di, X., Liu, H. X., Ban, X. J. X., Yu, J. W., 2015. Submission to the DTA 2012 special issue: On the stability of a boundedly rational day-to-day dynamic. Networks Spat. Econ. 15(3),

537-557.

Dong, J.X., Song, D.P., 2009. Container fleet sizing and empty repositioning in liner shipping systems. Transp. Res. Part E 45, 860–877.

Friesz, T. L., Bernstein, D., Mehta, N. J., Tobin, R. L., Ganjalizadeh, S., 1994. Day-to-day dynamic network disequilibria and idealized traveler information systems. Oper. Res. 42(6), 1120-1136.

Forrester, A.I.J., Keane, A.J., 2009. Recent advances in surrogate-based optimization. Prog. Aerosp. Sci. 45, 50–79.

Fu, X., Lam, W.H., 2018. Modelling joint activity-travel pattern scheduling problem in multi-modal transit networks. Transportation 45(1), 23-49.

Gu, X., Abdel-Aty, M., Xiang, Q., Cai, Q., Yuan, J., 2019. Utilizing UAV video data for in-depth analysis of drivers' crash risk at interchange merging areas. Accid. Anal. Prev. 123, 159-169.

Guo, R.-Y., Yang, H., Huang, H.-J., Tan, Z., 2016. Day-to-day flow dynamics and congestion control. Transp. Sci. 50, 982–997.

Guo, X., Liu, H.X., 2011. Bounded rationality and irreversible network change. Transp. Res. Part B 45(10), 1606-1618.

Han, Z.-H., Zhang, K.-S., 2012. Surrogate-based optimization, in: Roeva, O. (Ed.), Real-World Applications of Genetic Algorithms. IntechOpen, pp. 333–362.

Hazelton, M.L., 2002. Day-to-day variation in Markovian traffic assignment models. Transp. Res. Part B 36(7), 637-648.

Hazelton, M. L., Watling, D.P., 2004. Computation of equilibrium distributions of Markov traffic-assignment models. Transp. Sci. 38(3), 331-342.

Hazelton, M.L., Parry, K., 2016. Statistical methods for comparison of day-to-day traffic models. Transp. Res. Part B 92, 22-34.

He, X., Chen, X., Xiong, C., Zhu, Z., Zhang, L., 2017. Optimal time-varying pricing for toll roads under multiple objectives: A simulation-based optimization approach. Transp. Sci. 51, 412–426.

He, X., Guo, X., Liu, H.X., 2010. A link-based day-to-day traffic assignment model. Transp. Res. Part B 44, 597–608.

He, X., Liu, H.X., 2012. Modeling the day-to-day traffic evolution process after an unexpected network disruption. Transp. Res. Part B 46, 50–71.

Li, L., Zhang, J., Wang, Y., Ran, B., 2018. Missing value imputation for traffic-related time series data based on a multi-view learning method. IEEE T. Intell. Transp., in press. DOI: 10.1109/TITS.2018.2869768.

Liu, Y., Liu, Z., Jia, R., 2019a. DeepPF: A deep learning based architecture for metro passenger flow prediction. Transp. Res. Part C 101, 18-34.

Liu, Z., Wang, S., Zhou, B., Cheng, Q., 2017. Robust optimization of distance-based tolls in a network considering stochastic day to day dynamics. Transp. Res. Part C 79, 58-72.

Horowitz, J.L., 1984. The stability of stochastic equilibrium in a two-link transportation network. Transp. Res. Part B 18(1), 13-28.

Hu, T. Y., Mahmassani, H. S., 1997. Day-to-day evolution of network flows under real-time information and reactive signal control. Transp. Res. Part C, 5(1), 51-69.

Iman, R.L., Helton, J.C., 1988. An investigation of uncertainty and sensitivity analysis techniques for computer models. Risk Anal. 8, 71–90.

Jones, D.R., Schonlau, M., Welch, W.J., 1998. Efficient global optimization of expensive black-box functions. J. Glob. Optim. 13, 455–492.

Kleijnen, J.P.C., 2017. Regression and kriging metamodels with their experimental designs in simulation: A review. Eur. J. Oper. Res. 256, 1–16.

Kleijnen, J.P.C., 2015. Design and analysis of Monte Carlo experiments (Second Edition). Springer.

Kleijnen, J.P.C., 2009. Kriging metamodeling in simulation: A review. Eur. J. Oper. Res. 192, 707–716.

Liu, W., Geroliminis, N., 2017. Doubly dynamics for multi-modal networks with park-and-ride and adaptive pricing. Transp. Res. Part B 102, 162–179.

Liu, Z., Wang, S., Zhou, B., Cheng, Q., 2017. Robust optimization of distance-based tolls in a network considering stochastic day to day dynamics. Transp. Res. Part C 79, 58–72.

Lophaven, S.N., Søndergaard, J., Nielsen, H.B., 2002. DACE A Matlab kriging toolbox, IMM Informatiocs and Mathematical Modelling.

Lotan, T., 1997. Effects of familiarity on route choice behavior in the presence of

information. Transp. Res. Part C 5(3-4), 225-243.

Lu, X., Gao, S., Ben-Elia, E., 2011. Information impacts on route choice and learning behavior in a congested network: experimental approach. Transportation Research Record 2243(1), 89-98.

Mahmassani, H.S., 1990. Dynamic models of commuter behavior: Experimental investigation and application to the analysis of planned traffic disruptions. Transp. Res. Part A 24, 465–484.

Mahmassani, H.S., Chang, G.L., 1986. Experiments with departure time choice dynamics of urban commuters. Transp. Res. Part B 20(4), 297-320.

Mahmassani, H.S., Chang, G.L., 1987. On boundedly rational user equilibrium in transportation systems. Transp. Sci. 21(2), 89-99.

Mahmassani, H.S., & Jou, R.C., 2000. Transferring insights into commuter behavior dynamics from laboratory experiments to field surveys. Transp. Res. Part A 34(4), 243-260.

McKay, M.D., Beckman, R.J., Conover, W.J., 1979. A comparison of three methods for selecting values of input variables in the analysis of output from a computer code. Technometrics 21, 239–245.

Meneguzzer, C., Olivieri, A., 2013. Day-to-day traffic dynamics: Laboratory-like experiment on route choice and route switching in a simple network with limited feedback information. Procedia - Soc. Behav. Sci. 87, 44–59.

Merchant, D.K., Nemhauser, G.L., 1978a. A model and an algorithm for the dynamic traffic assignment problems. Transp. Sci. 12(3), 183-199.

Merchant, D.K., Nemhauser, G.L., 1978b. Optimality conditions for a dynamic traffic assignment model. Transp. Sci. 12(3), 200-207.

Ministry of Public Security, 2016. Technical specifications for automatic recognition technology of motor vehicle license plate images, Public Safety Industrial Standard in China, GA/T 833-2016.

Mun, J. S., 2007. Traffic performance models for dynamic traffic assignment: an assessment of existing models. Transp. Rev. 27(2), 231-249.

Noordhoek, M., Dullaert, W., Lai, D.S.W., de Leeuw, S., 2018. A simulation-optimization approach for a service-constrained multi-echelon distribution network. Transp. Res. Part

E 114, 292–311.

Osorio, C., Bierlaire, M., 2013. A simulation-based optimization framework for urban transportation problems. Oper. Res. 61, 1333–1345.

Osorio, C., Nanduri, K., 2015a. Energy-efficient urban traffic management: A microscopic simulation-based approach. Transp. Sci. 49, 637–651.

Osorio, C., Nanduri, K., 2015b. Urban transportation emissions mitigation: Coupling high-resolution vehicular emissions and traffic models for traffic signal optimization. Transp. Res. Part B 81, 520–538.

Palisade Corporation, 2004. Guide to using @RISK: Risk analysis and simulation add-in for Microsoft Excel (Version 4.5).

Pan, Y., Chen, S., Qiao, F., Ukkusuri, S. V., Tang, K., 2019. Estimation of real-driving emissions for buses fueled with liquefied natural gas based on gradient boosted regression trees. Sci. Total Environ. 660, 741-750.

Parry, K., Hazelton, M.L., 2013. Bayesian inference for day-to-day dynamic traffic models. models. Transp. Res. Part B 50, 104-115.

Peeta, S., Ziliaskopoulos, A. K., 2001. Foundations of dynamic traffic assignment: The past, the present and the future. Networks Spat. Econ. 1(3-4), 233-265.

Pi, X., Ma, W., Qian, Z.S., 2019. A general formulation for multi-modal dynamic traffic assignment considering multi-class vehicles, public transit and parking. Transp. Res. Part C 104, 369-389.

Sacks, J., Welch, W.J., Mitchell, T.J., Wynn, H.P., 1989. Design and analysis of computer experiments. Stat. Sci. 4, 409–423.

Sheffi, Y., 1985. Urban transportation networks: equilibrium analysis with mathematical programming methods. Prentice-Hall, Inc., Englewood Cliffs, New Jersey.

Smith, M.J., 1984. The stability of a dynamic model of traffic assignment - an application of a method of Lyapunov. Transp. Sci. 18(3), 245-252.

Smith, M.J., & Wisten, M.B., 1995. A continuous day-to-day traffic assignment model and the existence of a continuous dynamic user equilibrium. Ann. Oper. Res. 60(1), 59-79.

Smith, M.J., Watling, D.P., 2016. A route-swapping dynamical system and Lyapunov function for stochastic user equilibrium. Transp. Res. Part B 85, 132-141.

Srinivasan, K.K., Mahmassani, H.S., 2003. Analyzing heterogeneity and unobserved structural effects in route-switching behavior under ATIS: a dynamic kernel logit formulation. Transp. Res. Part B 37(9), 793-814.

Szeto, W.Y., Lo, H.K., 2006. Dynamic traffic assignment: properties and extensions. Transportmetrica 2(1), 31-52.

Watling, D.P., Cantarella, G.E., 2013. Modelling sources of variation in transportation systems: theoretical foundations of day-to-day dynamic models. Transportmetrica B 1(1), 3-32.

Watling, D.P., Cantarella, G.E., 2015. Model representation & decision-making in an ever-changing world: the role of stochastic process models of transportation systems. Networks Spat. Econ. 15(3), 843-882.

Wu, J., Sun, H., Wang, D.Z.W., Zhong, M., Han, L., Gao, Z., 2013. Bounded-rationality based day-to-day evolution model for travel behavior analysis of urban railway network. Transp. Res. Part C 31, 73-82.

Xu, C., Wang, Y., Liu, P., Wang, W., Bao, J., 2018. Quantitative risk assessment of freeway crash casualty using high-resolution traffic data. Reliab. Eng. Syst. Safe., 169, 299-311.

Yang, F., Zhang, D., 2009. Day-to-day stationary link flow pattern. Transp. Res. Part B 43(1), 119-126.

Ye, H., Xiao, F., Yang, H., 2018. Exploration of day-to-day route choice models by a virtual experiment. Transp. Res. Part C 23, 679-699.

Ye, H., Yang, H., 2017. Rational behavior adjustment process with boundedly rational user equilibrium. Transp. Sci. 51(3), 968-980.

Zhan, X., Li, R., Ukkusuri, S. V, 2015. Lane-based real-time queue length estimation using license plate recognition data. Transp. Res. Part C 57, 85-102.

Zhang, F., Liu, W., 2019. Responsive bus dispatching strategy in a multi-modal and multi-directional transportation system: A doubly dynamical approach. Transp. Res. Part C, in press. https://doi.org/10.1016/j.trc.2019.04.005.

Zhang, W., Xu, W., 2017. Simulation-based robust optimization for the schedule of single-direction bus transit route: The design of experiment. Transp. Res. Part E 106, 203-230.

Zhou, B., Xu, M., Meng, Q., Huang, Z., 2017. A day-to-day route flow evolution process towards the mixed equilibria. Transp. Res. Part C 82, 210-228.